phism information content (PIC) (*8*) of the Sma2.6 RFLP is 0.58, raising the overall PIC of the D4S43 locus to an estimated 0.70. Thus, the marker should be informative in the majority of families for which presymptomatic diagnosis is attempted.

The predictive value of the D4S43 locus would be further enhanced if any of the RFLPs displayed a strong association with the disease gene due to linkage disequilibrium between the two loci. In this instance, presymptomatic diagnosis could potentially be extended to those "at risk" individuals who have too few living relatives for application of the linkage test. Such a result would also suggest that D4S43 and *HD* are in extremely close proximity. To test for linkage disequilibrium, we typed a collection of unrelated individuals affected by HD (*9*), along with their respective unaffected, and sometimes affected parents. The unaffected parents provide a control group for determining the frequency of individual alleles on normal chromosomes. Comparison of the parental genotypes with those of the affected offspring served to identify in most instances the particular allele inherited together with the HD gene in a given family. For all eight RFLPs, we observed no significant association between the defect and any specific allele ($P > 0.05$ in all cases). Furthermore, when alleles for the individual RFLPs were considered together, a minimum of ten different haplotypes were present on HD chromosomes. Thus, either the assumption that most affected individuals have inherited an HD defect of common origin is incorrect, or the D4S43 marker is not close enough to the defect to detect linkage disequilibrium without examining individuals from specific ethnic groups or geographic locations.

The position of D4S43 makes it the closest available marker to the HD gene, increasing both the accuracy and applicability of predictive testing. The absence of crossovers with HD, together with a physical localization within the terminal 3% of the short arm of chromosome 4, make D4S43 a suitable starting point for progressing toward the HD gene by chromosome walking, long-range physical mapping by pulsed field gel electrophoresis, and sophisticated directional cloning techniques such as chromosome "jumping." Although it is impossible to estimate the exact physical distance that separates the two loci, both are bracketed by D4S10 and the telomere within a region probably containing about 0.2% of the genome (*2*). With no crossovers detected between D4S43 and *HD*, the two independent coding sequences represented by the LCD cDNA, and a different cDNA isolated by means of S1.5, remain candidates for the site of the HD defect.

REFERENCES AND NOTES

1. J. B. Martin and J. F. Gusella, *N. Engl. J. Med.* **315**, 1267 (1986).
2. J. F. Gusella *et al.*, *Nature (London)* **306**, 234 (1983); J. Haines *et al.*, *Am. J. Hum. Genet.* **39**, A156 (1986); T. C. Gilliam *et al.*, *Cell* **50**, 565 (1987).
3. M. E. MacDonald *et al.*, *Genomics* **1**, 29 (1987); T. C. Gilliam *et al.*, *Nucleic Acids Res.* **15**, 1445 (1987); T. C. Gilliam *et al.*, unpublished results.
4. R. E. Tanzi *et al.*, *Science* **235**, 880 (1987); R. E. Tanzi *et al.*, in preparation.
5. The program LINKMAP from the LINKAGE package [version 3.5; G. M. Lathrop, J. M. Lalouel, C. Julier, C. Ott, J. Ott, *Am. J. Hum. Genet.* **37**, 482 (1985)] was used to calculate lod scores for various potential locations of the D4S43 marker relative to fixed positions for two other DNA loci, D4S10 and *RAF2*. The latter is a pseudogene of the c-*raf* proto-oncogene and has previously been physically and genetically mapped in 4p16.1, 21 cM proximal to D4S10 (*2, 3*). The multipoint analysis yielded peak lod scores for positions of D4S43 distal to D4S10, between D4S10 and *RAF2*, and proximal to *RAF2* as follows: $z = 32.0$ at 4 cM distal to D4S10, $z = 26.5$ at 5 cM proximal to D4S10 and 16 cM distal to *RAF2*, and $z = 8.7$ at 19 cM proximal to *RAF2*.
6. The three pedigrees included in the lod score analysis were known to contain a minimum of five recombinations between D4S10 and *HD* that were not detected by D4S43. In addition, individual recombinations between D4S10 and *HD* in five other families were similarly not detected by D4S43, but these pedigrees were not included in the computer analysis since only selected individuals had been typed.
7. Y. Nakamura *et al.*, *Science* **235**, 1616 (1987).
8. D. Botstein, R. L. White, M. Skolnick, R. Davis, *Am. J. Hum. Genet.* **32**, 314 (1980).
9. Each RFLP was typed in 35 to 70 affected HD individuals and their respective unaffected parents. The distribution of alleles on the chromosomes carrying the HD gene was tested by χ^2 analysis for deviation from the expected allele frequencies based on normal chromosomes.
10. A. Poustka *et al.*, *Proc. Natl. Acad. Sci. U.S.A.* **81**, 4129 (1984).
11. H. R. Rackwitz *et al.*, *Gene* **30**, 195 (1984).
12. P. G. Sealey, P. A. Whittaker, E. M. Southern, *Nucleic Acids Res.* **13**, 1905 (1985).
13. Two-factor lod score analysis was carried out by means of the MLINK program of the LINKAGE package and the LIPED program [J. Ott, *Am. J. Hum. Genet.* **26**, 588 (1974); *Am. J. Hum. Genet.* **28**, 528 (1976)] with an age of onset correction for the HD phenotype [S. E. Hodge, L. A. Morton, S. Tidemam, K. K. Kidd, M. A. Spence, *ibid.* **31**, 761 (1979)].

14. Supported by NINCDS grants NS16367 (Huntington's Disease Center Without Walls), NS22031, and NS20012 and by grants from the McKnight Foundation, Hereditary Disease Foundation, and Julieanne Dorn Fund for Neurological Research. J.F.G. is a Searle Scholar of the Chicago Community Trust. T.C.G. and M.E.M. were supported by the Anna Mitchell Fellowship and Grace E. Neuman Fellowship, respectively, from the Hereditary Disease Foundation. J.L.H. is supported by PHS postdoctoral training grant T32DE07043. S.V.C. received a fellowship from the National Huntington's Disease Association. B.A.A. and W.L.W. received support from the Huntington's Disease Society of America and the Wills Foundation.

31 July 1987; accepted 11 September 1987

Long-Term Neuropathological and Neurochemical Effects of Nucleus Basalis Lesions in the Rat

GARY W. ARENDASH,* WILLIAM J. MILLARD, ADRIAN J. DUNN, EDWIN M. MEYER

The long-term effects of excitotoxic lesions in the nucleus basalis magnocellularis of the rat were found to mimic several neuropathological and chemical changes associated with Alzheimer's disease. Neuritic plaque–like structures, neurofibrillary changes, and neuronal atrophy or loss were observed in the frontoparietal cortex, hippocampus, amygdala, and entorhinal cortex 14 months after the lesions were made. Cholinergic markers in neocortex were reduced, while catecholamine and indoleamine metabolism was largely unaffected at this time. Bilateral lesions of the nucleus basalis magnocellularis increased somatostatin and neuropeptide Y in the cortex of the rat by at least 138 and 284 percent, respectively, suggesting a functional interaction between cholinergic and peptidergic neurons that may differ from that in Alzheimer's disease.

ALZHEIMER'S DISEASE (AD), THE most common cause of dementia in the elderly, is consistently associated with a loss or dysfunction of cholinergic neurons in the nucleus basalis of Meynert (NBM) (*1, 2*) that project to the cerebral cortex. Other transmitters such as the peptides somatostatin (SS) and neuropeptide Y (NPY) are also reduced in the cortices of some brains from patients with AD (*3*), suggesting their involvement in the disease process. Neuropathologically, AD is characterized by cerebral atrophy due to substantial neuronal losses primarily in two brain regions important for cognitive functioning—the cerebral cortex and hippocampus (*4*). Within these regions of AD brains there are many neuritic plaques and neurofibrillary tangles (*5*).

G. W. Arendash, Section of Physiology and Development, Department of Biology, University of South Florida, Tampa, FL 33620.
W. J. Millard, Department of Pharmacodynamics, University of Florida, Gainesville, FL 32610.
A. J. Dunn, Department of Neuroscience, University of Florida, Gainesville, FL 32610.
E. M. Meyer, Department of Pharmacology, University of Florida, Gainesville, FL 32610.

*To whom correspondence should be sent.

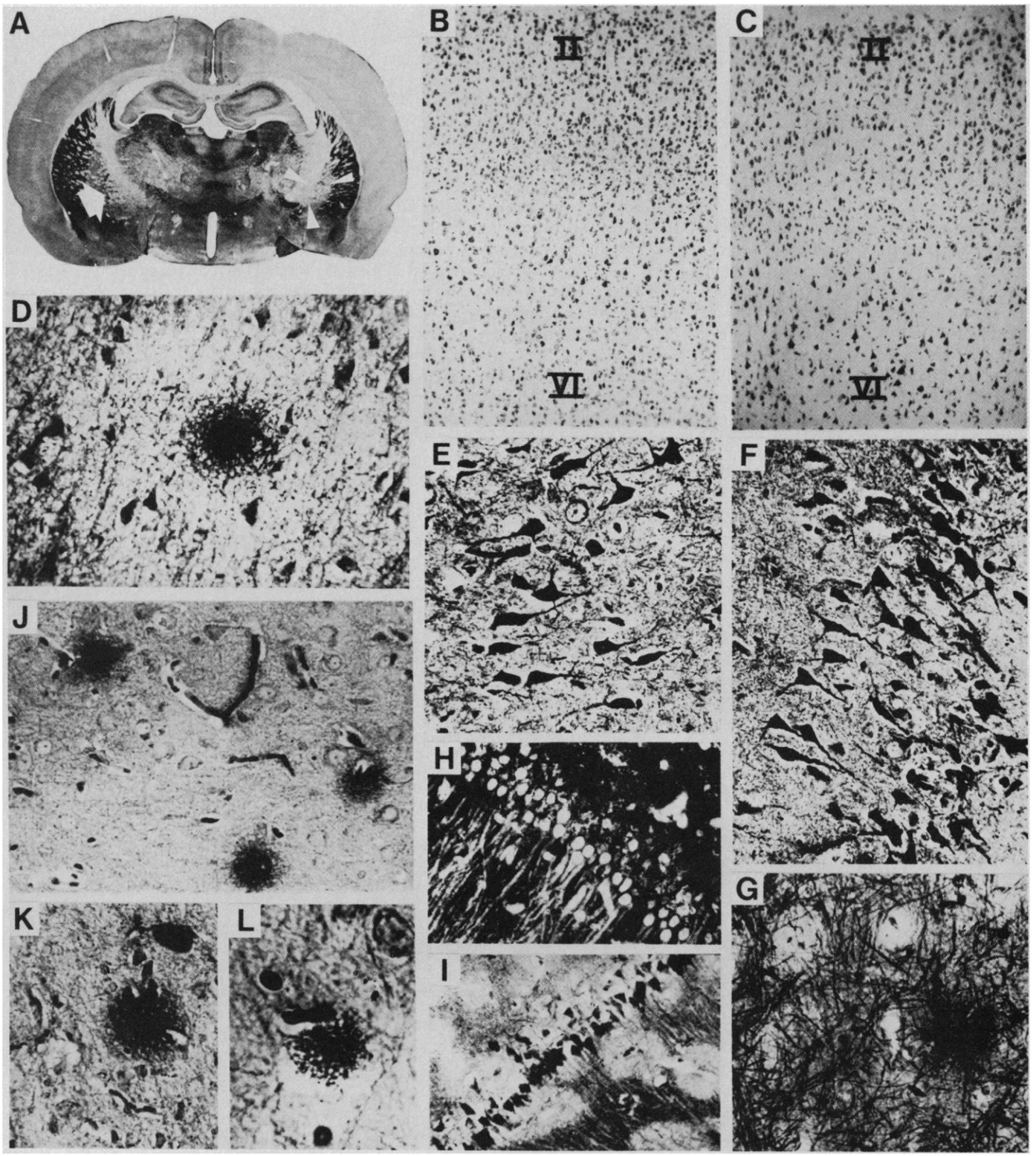

Fig. 1. (**A**) Coronal section of an animal receiving a unilateral nBM infusion of ibotenic acid. The section was stained for acetylcholinesterase (*34*) to visualize the intact nBM (arrowhead) and extent of neuronal destruction on the ibotenic acid-infused side (triangles). (**B** and **C**) Thionine-stained parietal cortex on the control (B) and lesioned (C) side of an animal given a unilateral nBM lesion 14 months earlier (×100). (**D**) A neuritic plaque–like structure and heavily silver-impregnated neurons in parietal cortex after nBM lesioning (×400). (**E**) Silver-impregnated neurons in the basolateral nucleus of the amygdala after nBM lesions (×400). (**F**) Silver-stained, atrophic neurons within layers II and III of the entorhinal cortex 14 months after nBM lesioning (×400). (**G**) A plaque-like structure in the silver-stained dorsal hippocampus 14 months after nBM lesioning (×400). (**H** and **I**) The pyramidal cell layer of the dorsal hippocampus on control (H) and lesioned (I) sides from a unilaterally lesioned rat (×400). (**J**) Three plaque-like structures in the frontolateral cortex after nBM lesioning (×400). (**K** and **L**) Neuritic plaque–like structures in silver-stained frontal (×400) and parietal (×1000) cortex, respectively, after nBM lesioning.

Although several attempts have been made to mimic the degeneration and atrophy of NBM cholinergic neurons in AD by lesioning the analogous nucleus basalis magnocellularis (nBM) in the rat, little is known about the long-term pathological and chemical effects of these lesions. We now report that several characteristics of AD are observed 14 months after nBM lesions.

Two-month-old male Sprague-Dawley rats were infused with the neurotoxin ibotenic acid into the nBM either unilaterally or bilaterally (*6*). Those animals with bilateral infusions were tested in a variety of learning- and memory-related tasks over the ensuing 7-month period and were killed 14 months after lesioning (*7*). Prefrontal, frontal, and parietal cortices from the right hemisphere of each animal were used to assay catecholamine and serotonin metabolites (*8*), cholinergic markers (*9*), and neuropeptides (*10*), respectively. The left hemisphere from these bilaterally lesioned animals was processed histologically (*11*), and brain sections were stained with either (i) silver impregnation (*12*) to visualize neuronal fibers and neurofibrils, (ii) Congo red (*13*) to identify amyloid deposits, or (iii) thionine to determine neuronal densities (*14*). Brains from animals with unilateral nBM lesions were also removed 14 months after lesioning, histologically sectioned, and stained according to the three methods just described.

Consistent with earlier nBM lesion studies (*6, 15*), bilaterally lesioned rats were deficient in learning and/or memory for a variety of tasks including multiple trial passive avoidance, two-way active avoidance, Lashley III maze performance, and pole-jumping active avoidance (*16*). Histological examination of brain sections from these lesioned animals killed at 14 months revealed a restricted gliosis (with essentially no surviving neurons) that encompassed the entire ventromedial globus pallidus containing the nBM (Fig. 1A) (*17*). No damage to fibers of passage was observed.

Fourteen months after bilateral nBM lesions, significant decreases were observed in cerebral cortical choline acetyltransferase activity, high-affinity choline transport, and coupled [^{3}H]acetylcholine synthesis in isolated nerve terminals (Table 1). Low-affinity choline transport was not affected (*18*). Monoamine concentrations in the prefrontal cortex were largely unaffected by nBM lesions (Table 1). However, there was a small (18%), but statistically significant, decrease in cortical norepinephrine concentrations in lesioned animals (*19*). SS and NPY levels in parietal cortex were elevated by 138 and 284%, respectively, 14 months after lesions (Fig. 2). The enhancement in cortical concentrations of both peptides is consistent with observations showing neuronal colocalization of these peptides in the rat as well as in human cerebral cortex (*20*). Although these results suggest a functional relation between nBM neurons projecting to the cortex and SS- and NPY-containing neurons, the mechanism by which nBM lesions increase the concentrations of these peptides remains obscure. Acetylcholine is a potent secretagogue of SS in the rat cortex (*21*) and NPY in the adrenal medulla (*22*). Thus, it is conceivable that the loss of cholinergic input from the nBM eventually leads to the accumulation of these peptides in the cortex.

Bilaterally lesioned animals suffered substantial neuronal losses (from 14 to 27%) in all layers of the frontoparietal cortex investigated (Table 2), with particularly marked losses in the parietal cortex. Even rats given unilateral nBM lesions experienced neuronal losses (from 27 to 41%) in various frontoparietal cortex layers on the lesioned side compared to the unlesioned side (Fig. 1, B and C). Fourteen months after nBM lesions, many surviving cortical neurons were atrophied or stained intensely by silver impregnation or both (Fig. 1D), particularly in the dorsomedial and lateral cortex. Probably because of cortical cell losses after such lesioning, fiber staining in the frontoparietal cortex was lighter than controls and often had a "spongy" appearance (with vacuolation of tissue). No such changes in fiber staining were seen within cortical areas that do not receive nBM cholinergic projections (cingulate cortex, pyriform cortex, and posterior neocortex). Moreover, a large number of heavily silver impregnated, dystrophic neurons were observed in the basolateral nucleus of the amygdala (Fig. 1E), which receives a cholinergic projection from the nBM (*23*) and is involved neuropathologically in AD (*24*).

Table 1. Cortical cholinergic and monoaminergic markers 14 months after bilateral nBM lesions. Abbreviations: CAT, choline acetyltransferase; HACT, high-affinity choline transport; LACT, low-affinity choline transport; ACh, acetylcholine; NE, norepinephrine; MHPG, 3-methoxy-4-hydroxyphenylglycol; DA, dopamine; DOPAC, dihydroxyphenolacetic acid; 5-HT, serotonin; 5-HIAA, 5-hydroxyindoleacetic acid. Data are expressed as picomoles per milligram of wet weight tissue per time for cholinergic markers and nanograms per milligram of wet weight tissue for monoaminergic markers.

Marker	Control	Lesioned
Cholinergic markers	$n = 5$	$n = 4$
CAT activity per (pmol/mg per 15 minutes)	2.08 ± 0.16	1.44 ± 0.10*
HACT (pmol/mg per 2 minutes)	23.8 ± 2.1	17.4 ± 1.3*
LACT (pmol/mg per 2 minutes)	31.6 ± 4.0	27.9 ± 1.0
ACh synthesis (pmol/mg per 2 minutes)	10.8 ± 1.8	5.2 ± 1.6*
Monoamine markers (ng/mg)	$n = 3$	$n = 4$
NE	0.503 ± 0.037	0.411 ± 0.005*
MHPG	0.106 ± 0.005	0.120 ± 0.014
DA	0.094 ± 0.016	0.083 ± 0.008
DOPAC	0.049 ± 0.008	0.040 ± 0.002
5-HT	0.389 ± 0.073	0.336 ± 0.054
5-HIAA	0.373 ± 0.026	0.344 ± 0.025
Tryptophan	3.38 ± 0.38	3.34 ± 0.26

*Significantly different from controls ($P < 0.05$; t test).

Table 2. Neuronal densities in cerebral cortex at 14 months after bilateral nBM lesioning. For each animal, a mean neuronal density from five representative brain sections was used to compute the mean ± SEM for both groups.

Cortical area	Neuronal density (neurons/0.09 mm^2)		
	Control	Lesioned	Decrease (%)
Anterior frontal			
Layer II	50.6 ± 1.7	39.0 ± 3.0**	22
Layer III	30.4 ± 0.9	26.2 ± 0.6**	14
Layer VI	39.8 ± 2.1	31.4 ± 2.4*	21
Posterior frontal			
Layer II	50.6 ± 3.2	42.3 ± 2.3	17
Layer III	33.4 ± 2.2	27.0 ± 1.0*	21
Layer VI	40.0 ± 1.9	29.2 ± 2.2**	27
Anterior parietal			
Layer II	73.2 ± 3.1	55.8 ± 1.7***	24
Layer III	44.4 ± 0.9	32.6 ± 2.0***	27
Layer VI	55.0 ± 0.7	44.2 ± 0.7***	20

*$P < 0.05$, **$P < 0.025$, ***$P < 0.005$ (t test; $n = 5$ for both lesioned and control groups).

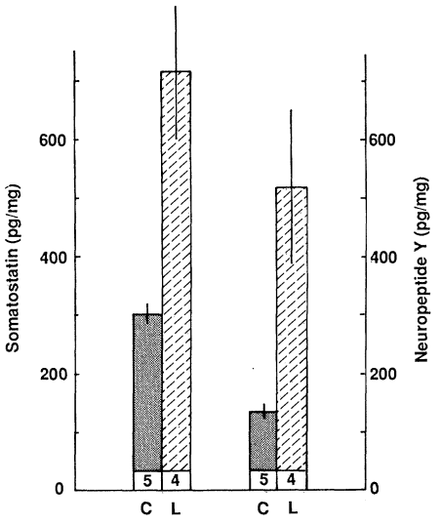

Fig. 2. Somatostatin and NPY concentrations (picograms per milligram wet weight) in parietal cortex from animals given bilateral nBM lesions or sham surgery 14 months prior to being killed. Concentrations of both peptides were significantly different in lesioned (L) compared to sham-lesioned animals (C) ($P < 0.001$; t test). The increased concentrations of these two neuropeptides in the cortex would have been even more dramatic (180 and 387%, respectively) if not for one lesioned animal that had normal amounts of both peptides and normal cortical CAT activity. Error bars are SEM and the number of animals in each group is indicated at the bottom of each bar.

AD is characterized by a degeneration of the entorhinal cortex (primarily layers II and III) that includes cell losses, neuronal atrophy, and the presence of neurofibrillary tangles (*25*). Similar entorhinal pathology was seen in rats that received nBM lesions 14 months earlier, with heavily silver-impregnated, atrophied neurons observed in layers II and III of entorhinal cortex. Moreover, hippocampal fiber staining often appeared spongy and was consistently lighter after nBM lesions (Fig. 1, G and I). Neuronal losses in the various strati of the dorsal hippocampus were evident, as were extensive numbers of silver-stained neurons surviving in a severely atrophic state (Fig. 1, H and I). Also after nBM lesions, neuritic plaque–like structures were occasionally seen in the cerebral cortex and hippocampus (Fig. 1, D, E, J, K, and L); these structures resembled immature plaques found in human and monkey brains (*5, 26, 27*) in that they consisted of degenerative neuronal terminals and glial elements, with no associated amyloid deposits (*28*). Congo red staining in cerebral cortex did not show any abnormalities.

The slow development of neuropathological changes in neocortex, amygdala, entorhinal cortex, and hippocampus after nBM lesions suggests a mechanism involving anterograde transneuronal degeneration due to a loss of cholinergic activity. Anterograde transneuronal degeneration has been well documented in human, monkey, and rat brains after neuronal lesions (*29*). Because nBM cholinergic neurons do not project directly to either the entorhinal cortex or hippocampus, the degenerative changes in these two regions may be due to subsequent transneuronal effects occurring in response to altered neocortical input to the entorhinal cortex, which in turn causes dysfunctional entorhinal input to hippocampus via the perforant pathway. Such a cascade of transneuronal events may underlie the degenerative changes in entorhinal cortex and hippocampus observed in AD. In this context, the entorhinal cortex provides the primary relay of neocortical information to the hippocampus via the perforant pathway, which becomes dysfunctional in this disease (*25, 30*).

The heavily silver-stained, atrophic neurons found in all four forebrain regions are very similar to the neurons within these same regions of AD brains (*5, 24, 25, 31*). Whether the neurofibrillary changes in our nBM lesioned rats are due to the presence of abnormal paired helical filaments, as is the case in AD, or to an accumulation of normal neurofilamentous protein is unknown. The induction of neuritic plaque–like structures supports a prime role for degeneration of the nBM cholinergic projections in neuritic plaque pathogenesis. Studies in primates, showing the presence of cholinergic terminals in plaques (*27, 32*) and a correlation between nBM cell losses and cortical plaque densities (*33*), are consistent with this premise.

Our data demonstrate that the loss of projections from the nBM to the cerebral cortex, presumably cholinergic, is sufficient to cause a variety of neurochemical, behavioral, and neuropathological effects associated with AD. None of the neuropathology we have described was observed before 5 months after the nBM lesions were made. Similarly, the dramatic enhancement in cortical SS and NPY levels was not present immediately after the nBM lesions. The time course for the appearance of these changes may indicate that degeneration of NBM cholinergic neurons in humans developing AD begins long before similar changes are obvious in their brains. Our data suggest that a primary lesion in the human NBM may similarly result in a variety of transneuronal effects throughout the telencephalon.

Because the long-term nBM-lesioned rat displays cognitive deficits (*6, 15*), certain neurochemical dysfunctions, and much of the neuropathology associated with AD, we suggest that it is a useful animal model for studying cholinergic-based dysfunction of the disease.

REFERENCES AND NOTES

1. R. T. Bartus *et al.*, *Science* **217**, 408 (1982); J. T. Coyle, D. L. Price, M. R. DeLong, *ibid.* **219**, 1184 (1983); F. Crews *et al.*, in *Treatment Development Strategies for Alzheimer's Disease*, T. Crook, R. Bartus, S. Ferris, S. Gershon, Eds. (Powley, Madison, CT, 1986), pp. 385–419.
2. P. J. Whitehouse *et al.*, *Science* **215**, 1237 (1982); R. Pearson *et al.*, *Brain Res.* **289**, 375 (1983); T. Nagai, P. McGeer, J. Peng, E. McGeer, C. Dolman, *Neurosci. Lett.* **36**, 195 (1983).
3. P. Davies, R. Katzman, R. D. Terry, *Nature (London)* **288**, 279 (1980); M. Rossor, P. Emson, C. Montjoy, M. Roth, L. Iversen, *Neurosci. Lett.* **20**, 373 (1980); P. Davies and R. Terry, *Neurobiol. Aging* **2**, 9 (1981); I. Ferrier *et al.*, *J. Neurol. Sci.* **62**, 159 (1983); J. Candy *et al.*, *ibid.* **71**, 315 (1986); M. F. Beal *et al.*, *Ann. Neurol.* **20**, 282 (1986).
4. R. Terry *et al.*, *Ann. Neurol.* **10**, 184 (1981); R. Terry and R. Katzman, in *The Neurobiology of Aging*, R. Katzman and R. Terry, Eds. (Davis, Philadelphia, 1983), pp. 51–84; M. Mann *et al.*, *J. Neurol. Neurosurg. Psychiatry* **49**, 310 (1986).
5. B. Tomlinson, G. Blessed, M. Roth, *J. Neurol. Sci.* **11**, 215 (1970); B. Tomlinson, in *Dementia*, C. E. Wells, Ed., vol. 15 of *Contemporary Neurology* (Davis, Philadelphia, ed. 2, 1977), pp. 113–153; H. Wisniewski and G. Mertz, in *Biological Aspects of Alzheimer's Disease*, R. Katzman, Ed. (Banbury Report, no. 15, Cold Spring Harbor Laboratory, Cold Spring Harbor, NY, 1983), pp. 145–153; H. Wisniewski, G. Merz, G. Wen, K. Iqbal, I. Grundke-Iqbal, in *Senile Dementia of the Alzheimer Type*, J. T. Hutton and A. D. Kenny, Eds. (Liss, New York, 1985), vol. 18, pp. 263–274.
6. G. W. Arendash, P. N. Strong, P. R. Mouton, in *Senile Dementia of the Alzheimer Type*, J. T. Hutton and A. D. Kenny, Eds. (Liss, New York, 1985), vol. 18, pp. 351–376. Ibotenic acid was dissolved in phosphate-buffered saline (*p*H 7.4) at a concentration of 5 mg/ml, and 1 μl was infused at two sites within each nBM according to the stereotaxic atlas of J. Konig and A. Klippel [*The Rat Brain: A Stereotaxic Atlas of the Forebrain and Lower Parts of the Brain Stem* (William and Wilkins, Baltimore, 1963)]; the second infusion was 0.8 mm dorsal to the first.
7. Animals were decapitated and their brains were immediately removed for biochemical and histological analyses. Dissections were performed according to the method of J. Glowinski and L. L. Iversen [*J. Neurochem.* **13**, 655 (1966)].
8. Monoamines and catabolites were measured by high-performance liquid chromatography with electrochemical detection [A. J. Dunn *et al.*, *Behav. Neural Biol.* **46**, 410 (1986)].
9. High-affinity choline uptake, low-affinity choline uptake, and acetylcholine synthesis were measured in synaptosomes prepared from the frontal cortex [E. M. Meyer and S. P. Baker, *Life Sci.* **39**, 1307 (1986)], as was CAT activity [E. Meyer *et al.*, *Mech. Ageing Dev.* **30**, 221 (1985)]. [^{3}H]Choline was purchased from NEN Research Products (Boston, MA).
10. Parietal cortex was weighed before adding 1 ml of cold 2*N* acetic acid and placing in boiling water for 5 minutes. Samples were homogenized by sonication, frozen, thawed, and centrifuged. Aliquots were lyophilized and reconstituted for radioimmunoassay. Double antibody radioimmunoassays for SS and NPY were performed, respectively, by the methods of M. A. Arnold *et al.* [*J. Neurosci.* **2**, 674 (1982)] and M. F. Beal *et al.* [*Neurosci. Lett.* **64**, 69 (1986)]. Iodinated NPY was obtained from NEN Research Products (Boston, MA), and the standard for the latter assay was porcine NPY (Peninsula, Belmont, CA). Intra-assay variabilities for the SS and NPY assays were 3.1 and 4.0%, respectively; sensitivities were 6 and 5 pg per tube, respectively.
11. Half brains were placed in 10% neutral buffered formalin for several days, then embedded in paraffin and serially sectioned at 8 μm (for silver staining) and 10 μm (for Congo red and thionine staining). Two 8-μm sections were collected for every 10-μm section collected.
12. B. Lloyd *et al.*, *J. Histotechnol.* **8**, 155 (1985).
13. H. Puchtler, F. Sweat, M. Levine, *J. Histochem.*

Cytochem. **10**, 355 (1962).
14. Five 10-μm sections (separated by at least 42 μm) were selected for each cortical area analyzed. Neurons within layers II, III, and VI of the dorsolateral neocortex were counted at ×600 by utilizing a grid containing four squares, which was mounted in the microscope eyepiece. Neurons were counted only if they contained a distinct nucleolus and only if more than half of the cell body was within the boundaries of the grid. Mean neuronal densities for each animal were used to compute the mean ± SEM for lesion and control groups. One-way analysis of variance was used to determine significant differences between groups.
15. G. LoConte, L. Bartolini, F. Casamentia, I. Marconcini-Pepeu, G. Pepeu, *Pharmacol. Biochem. Behav.* **17**, 933 (1982); C. Flicker, R. Dean, D. Watkins, S. Fisher, R. Bartus, *ibid.* **18**, 973 (1983); S. Dunnett *et al.*, *Neuroscience* **16**, 787 (1985); B. Knowlton *et al.*, *Brain Res.* **345**, 315 (1985); B. Dubois, W. Mayo, Y. Agid, M. LeMoal, H. Simon, *ibid.* **338**, 249 (1985); D. Hepler, D. Olton, G. Wenk, J. Coyle, *J. Neurosci.* **5**, 866 (1985).
16. P. N. Strong, E. M. Meyer, P. R. Mouton, G. W. Arendash, in preparation.
17. Our previous histological analysis of acetylcholinesterase-stained brain sections (*6*) revealed that the vast majority of large acetylcholinesterase-positive neurons within the nBM are destroyed by ibotenic acid infusions.
18. Cortical cholinergic activity remaining after nBM lesioning may be due to intrinsic cholinergic neurons in rodent, but not primate, cerebral cortex. To minimize the influence of these intrinsic cholinergic perikarya, we measured cholinergic markers in isolated nerve terminals.
19. It is not obvious why such an effect should be observed in nBM-lesioned animals, and, indeed, we have not observed this effect at any earlier time point (2 or 10 months) after nBM lesions nor has such an effect been reported in the literature. This effect may be spurious and not replicable. Alternatively, this nBM lesion–induced decrease in cortical norepinephrine (NE) levels may indicate that a relation exists between loss of nucleus basalis cholinergic neurons and a loss or dysfunction of NE neurons originating from the locus ceruleus, which provide noradrenergic innervation to the neocortex. Involvement of such NE neurons in AD is implicated from studies showing AD brains to have a marked loss of NE neurons within the locus ceruleus [L. L. Iversen *et al.*, *Neurosci. Lett.* **39**, 95 (1983)] and decreased NE concentrations in neocortex [R. Adolfsson *et al.*, *Br. J. Psychiatry* **135**, 216 (1979); D. Mann *et al.*, *J. Neurol. Neurosurg. Psychiatry* **45**, 113 (1982)].
20. S. R. Vincent *et al.*, *Nature (London)* **298**, 65 (1982); B. Chronwall, T. Chase, T. O'Donohue, *Neurosci. Lett.* **52**, 213 (1984); E. Jones and S. Stewart, *Res. Publ. Assoc. Res. Nerv. Ment. Dis.* **64**, 163 (1986).
21. R. Robbins, R. Sutton, S. Reichlin, *Brain Res.* **234**, 377 (1982).
22. T. Hesum, E. Majawe, L. Russett, H.-Y. T. Yang, *Soc. Neurosci. Abstr.* **12**, 997 (1986).
23. O. Ottersen, *J. Comp. Neurol.* **194**, 267 (1980); M. Mesulam, E. Mufson, B. Wainer, A. Levy, *Neuroscience* **11**, 1185 (1983).
24. D. Price *et al.*, *Ann. N.Y. Acad. Sci.* **396**, 145 (1982); A. Herzog and T. Kemper, *Arch. Neurol. (Chicago)* **37**, 625 (1980).
25. B. T. Hyman, G. W. Van Hoesen, A. R. Damasio, C. L. Barnes, *Science* **225**, 1168 (1984).
26. H. Wisniewski and R. Terry, *Prog. Neuropathol.* **2**, 1 (1973).
27. R. G. Struble, L. C. Cork, P. J. Whitehouse, D. L. Price, *Science* **216**, 413 (1982).
28. Since we have not seen any of these neuritic plaque–like structures in the brains of aged, 2-year-old rats (G. W. Arendash and J. Mazziotta, unpublished observations), they apparently do not occur spontaneously in the aging rat brain and would, therefore, appear to be the result of nBM lesioning.
29. W. Cowan, in *Contemporary Research Methods in Neuroanatomy*, W. J. H. Nauta and S. O. E. Ebbesson, Eds. (Springer-Verlag, New York, 1970), pp. 217–236.
30. B. Hyman, G. Van Hoesen, A. Damasio, *Soc. Neurosci. Abstr.* **12**, 944 (1986).
31. A. Hirano and H. Zimmerman, *Arch. Neurol. (Chicago)* **7**, 227 (1962); M. Ball, *Acta Neuropathol.* **37**, 111 (1978).
32. C. A. Kitt *et al.*, *Science* **226**, 1443 (1984).
33. T. Arendt, V. Bigl, T. Tennstedt, A. Arendt, *Neuroscience* **14**, 1 (1985).
34. M. Karnovsky and J. Roots, *J. Histochem. Cytochem.* **12**, 219 (1964).
35. Supported by a grant from the Alzheimer's Disease and Related Disorders Association and NIH grant HD 17933. We thank R. Ranhawa, J. Mazziotta, V. Dillela, P. Mouton, P. Jantzen, V. Panzarino, B. Moreshead, J. Judkins, and E. Hardwick for technical assistance and brain tissue analyses.

26 February 1987; accepted 31 July 1987

Environmental Correlates of Food Chain Length

FRÉDÉRIC BRIAND AND JOEL E. COHEN

In 113 community food webs from natural communities, the average and maximal lengths of food chains are independent of primary productivity, contrary to the hypothesis that longer food chains should arise when more energy is available at their base. Environmental variability alone also does not appear to constrain average or maximal chain length. Environments that are three dimensional or solid, however, such as a forest canopy or the water column of the open ocean, have distinctly longer food chains than environments that are two dimensional or flat, such as a grassland or lake bottom.

A COMMUNITY FOOD WEB (*1*) describes the feeding relations in a community of organisms. A trophic species (*2*) (hereinafter species) in a web is a collection of organisms that feed on a common set of organisms and are fed on by a common set of organisms. Species x is linked to species y when energy flows from x to y, that is, when y feeds on x. A chain is an energy path or sequence of links that starts at a species that eats no other species in the web and ends at a species that is eaten by no other species in the web. The length of a chain is the number of links it comprises. The mean chain length of a web is the arithmetic average of the lengths of all chains in the web.

Two major hypotheses and one empirical generalization have been proposed to relate chain lengths to environmental conditions. The first hypothesis, known as the "energetic hypothesis" (*3*), proposes that chain length is limited by the inefficiency with which energy is transmitted by predation and by the minimal energy requirements of predators. Limited available energy may make it impossible to support enough individuals to maintain a population, may make it impossible for individuals to find enough prey to survive, or may constrain chain length through other mechanisms. In its simple form, this hypothesis predicts that chains should be longer in ecosystems with higher primary productivity. It has been tested experimentally (*4*) and rejected for small artificial ecosystems, and it remains to be tested further experimentally. From a review of nine studies ranging from energetically impoverished to highly productive environments, Pimm (*5*) concluded that there was no evidence for food chains being longer in more productive habitats.

The second hypothesis, known as the dynamical stability hypothesis (*6*), is based on the finding in specific mathematical models of ecosystems that the longer the chains, the more severe the restrictions that must be imposed on the coefficients of the models for equilibrium to be feasible or stable. Further, in certain models, ecosystems with longer chains take longer to return to equilibrium once perturbed, so that webs with longer chains may be less likely to persist in nature. This hypothesis predicts that chains should be longer in ecosystems exempt from large perturbations. To our knowledge, there is no reported evidence for or against this hypothesis.

The empirical generalization (*7*), based on 34 webs, proposes that chains tend to be longer in three-dimensional than in two-dimensional environments. An environment is classified as having dimension 2 if it is essentially flat, like a grassland, the tundra, a sea or lake bottom, a stream bed, or the rocky intertidal zone. An environment is classified as having dimension 3 if it is solid, like the pelagic water column or a forest canopy. Webs from habitats integrating both flat and solid environments are considered as having "mixed" dimension.

To evaluate the relative influence on chain length of the primary productivity, the variability, and the dimensionality of the environment, we studied a collection of 113

F. Briand, World Conservation Center, International Union for the Conservation of Nature, CH-1196 Gland, Switzerland.
J. E. Cohen, Laboratory of Populations, Rockefeller University, New York, NY 10021.